

## Enhanced gut barrier integrity sensitizes colon cancer to immune therapy

Neal Bhutiani<sup>a</sup>, Qingsheng Li<sup>a</sup>, Charles D. Anderson<sup>a</sup>, Heather C. Gallagher<sup>b,c</sup>, Magdia De Jesus<sup>b,c</sup>, Rajbir Singh<sup>a</sup>, Venkatkrishna R. Jala<sup>a</sup>, Mostafa Fraig<sup>d</sup>, Tao Gu<sup>a</sup>, and Nejat K. Egilmez<sup>a</sup>

<sup>a</sup>Department of Microbiology and Immunology, School of Medicine, University of Louisville, Louisville, USA; <sup>b</sup>Department of Biomedical Sciences, University at Albany School of Public Health, One University Place Rensselaer Albany, USA; <sup>c</sup>Wadsworth Center, New York State Department of Health, David Axelrod Institute, Albany, USA; <sup>d</sup>Department of Pathology, School of Medicine, University of Louisville, Louisville, USA

### ABSTRACT

Oral IL-10 suppressed tumor growth in the APC<sup>min/+</sup> mouse/*Bacteroides fragilis* colon cancer model while a similar formulation of IL-12 exacerbated disease. In contrast, combined treatment with IL-10 and IL-12 resulted in near-complete tumor eradication and a significant extension of survival. The cytokines mediated distinct immunological effects in the gut, i.e. IL-10 diminished Th17 cell prevalence whereas IL-12 induced IFN $\gamma$  and enhanced CD8 + T-cell activity. Loss-of-function studies demonstrated that IL-12-driven CD8 + T-cell expansion was only partially responsible for the synergy, and that both the detrimental and the beneficial activities of IL-12 required IFN $\gamma$ . Examination of colon physiology in mice receiving single vs dual treatment revealed that exacerbation of disease by IL-12 monotherapy was associated with compromised gut barrier integrity whereas combined treatment reversed this effect, uncovering additional activity by the cytokines on the stroma. Further analysis showed that the stromal effects of IL-12 included a 6-fold increase in IL-10RA expression in the colon epithelium, linking the epithelial activity of the cytokines. Finally, dual but not monotherapy induced a 3-fold increase in tight junction protein levels in the colon, identifying the mechanism by which IL-10 blocked the detrimental effect of the IL-12-IFN $\gamma$  axis on barrier function without interfering with its beneficial immunological activity. These findings establish that the synergy between IL-12 and IL-10 was mediated by pleiotropic effects on the immune and the non-immune compartments and that the latter activity was critical to therapeutic outcome.

### ARTICLE HISTORY

Received 18 April 2018  
Revised 29 June 2018  
Accepted 3 July 2018

### KEYWORDS

IL-10; IL-12; IL-17; colon cancer; gut epithelial barrier

## Introduction

The recent clinical success of immune checkpoint inhibitors (ICI) represents a major breakthrough in cancer therapy.<sup>1</sup> At the same time, the effectiveness of ICI has not been uniform across different solid tumor types.<sup>2</sup> A major cancer type that remains highly resistant to ICI, and immune therapy in general, is mismatch repair (MMR)-proficient colorectal cancer (CRC).<sup>2,3</sup> While the mechanisms underlying resistance of MMR-proficient CRC to immune therapy are not fully understood the need for the development of new therapeutic approaches is clear.<sup>3</sup>


One distinction between CRC and most other cancers is the unusual characteristics of the tissue within which the cancer arises. The colon represents a unique environment due to the massive commensal microbiota burden and has evolved complex mechanisms to maintain the delicate balance between luminal bacteria and the immune cells that patrol the lamina propria (LP).<sup>4</sup> Breach of the single-cell thick epithelial barrier that separates the lumen from the LP can result in the loss of intestinal immune homeostasis and the development of severe inflammatory pathology.<sup>5</sup> Indeed, if such pathology becomes chronic, it can lead to development of cancer as

seen in colitis-associated cancer.<sup>6</sup> While inflammation that results from loss of epithelial barrier integrity can directly promote colon cancer, most sporadic CRC initially develops independent of chronic inflammation. However, once dysplasia develops, it will result in local compromise of the barrier and lead to what has been termed “tumor-elicited inflammation,” a process that in turn promotes the growth of established adenomas.<sup>7</sup> Therefore, chronic inflammation is tightly intertwined both with tumorigenesis and tumor progression in the colon. Consistent with this paradigm, a significant body of literature supports a major role for microbially-driven type 17 T-cell immunity (including Th17 and  $\gamma\delta$ T-cell subsets) in colon cancer.<sup>7–10</sup> Importantly, analysis of clinical CRC samples has revealed an inverse relationship in CD8+ cytotoxic T-lymphocyte (CTL)/Th17 cell ratio between MMR-deficient (high CTL, low Th17) and ICI-resistant MMR-proficient (low CTL, high Th17) tumors;<sup>11</sup> supporting the notion that the outcome of immune therapy in CRC may be dependent on the ability to alter the CTL – Th17 cell balance.

Interleukin-10 (IL-10) is a pluripotent immune regulatory cytokine that is central to the maintenance of immune homeostasis in mucosal tissues.<sup>12</sup> IL-10 converts immature blood

**CONTACT** Nejat Egilmez  [nejat.egilmez@louisville.edu](mailto:nejat.egilmez@louisville.edu)  505 S. Hancock St., Room 603, Louisville, Kentucky 40202, USA

N.K.E has ownership interest in TherapyX, Inc., which is developing PIN particle technology for commercial application. The remaining authors declare no competing financial interests.

 Supplemental data for this article can be accessed [here](#).

© 2018 The Author(s). Published with license by Taylor & Francis Group, LLC.

This is an Open Access article distributed under the terms of the Creative Commons Attribution-NonCommercial-NoDerivatives License (<http://creativecommons.org/licenses/by-nc-nd/4.0/>), which permits non-commercial re-use, distribution, and reproduction in any medium, provided the original work is properly cited, and is not altered, transformed, or built upon in any way.

monocytes to tolerogenic macrophages,<sup>13–15</sup> has direct suppressive effects on Th17 cell activity,<sup>16</sup> and conversely enhances conventional regulatory T-cell (cTreg) function.<sup>17</sup> A series of recent studies demonstrated that IL-10 directly activates antigen-experienced CD8+ cytotoxic T-lymphocytes independent of its suppressive effects on CD4 + T-effector and/or myeloid cell subsets.<sup>18–20</sup> Collectively, these properties have provided the rationale for our studies evaluating the therapeutic efficacy of a novel oral formulation of IL-10 in the treatment of intestinal polyposis<sup>21</sup> and, more recently, of colon cancer.<sup>22</sup> The findings revealed that oral IL-10 could suppress tumorigenesis in the above models via its dual activity on Th17 cells and CTL.

In this study, we tested whether oral IL-10 would be effective in eradicating established disease either alone or in combination with IL-12, a canonical Th1 cytokine that can directly activate tumor-associated CTL.<sup>23</sup> The results demonstrate potent synergy between IL-10 and IL-12, involving pleiotropic effects on immune cells and the gut epithelium, with the latter activity being critical to overall therapeutic efficacy.

## Results

Previous studies demonstrated that oral administration of a slow-release biodegradable particulate formulation of IL-10 suppressed intestinal polyposis in APC<sup>min/+</sup> mice and early tumorigenesis in the APC<sup>min/+</sup>/*B fragilis* compound colon cancer model.<sup>21,22</sup> We wanted to determine whether this approach would be effective in the treatment of established disease. To this end, APC<sup>min/+</sup> mice were inoculated with *B fragilis* and were allowed to develop tumors prior to the initiation of therapy. They were then administered IL-10 for 3 weeks, and colon tumor burden as well as histologic grade were analyzed. The results demonstrate that short-term treatment reduced tumor burden by 3-fold (Figure 1A) coupled with a modest decrease in maximum tumor diameter (Figure 1B). In contrast, treatment did not affect tumor histopathology (Figure 1C).

IL-10 suppresses colon tumorigenesis via its ability to reduce the prevalence of IL-17-producing T-cells with concurrent enhancement of CTL cytotoxicity.<sup>22</sup> We therefore hypothesized that adding IL-12 to the treatment regimen could further augment the functional balance in favor of

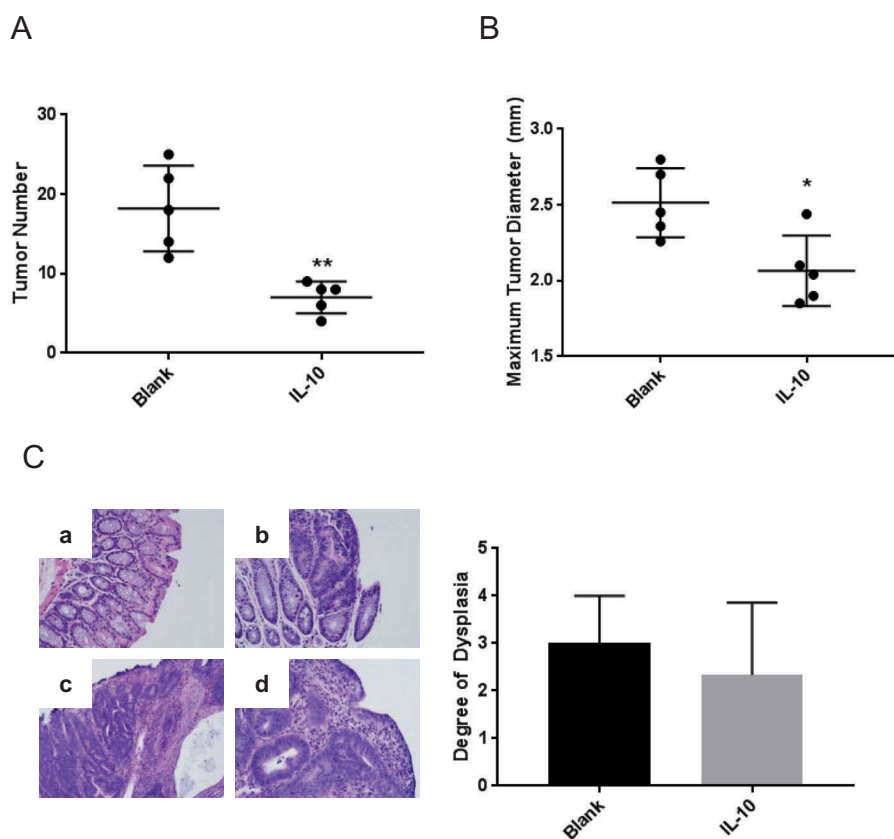


**Figure 1.** Oral IL-10 reduces tumor burden in mice with established disease. (A, B) Colon tumor number and maximum diameter. APC<sup>min/+</sup> mice were treated with oral particle-based therapy (either blank particles or particles loaded with recombinant murine IL-10) for 3 weeks beginning 4 weeks after enterotoxigenic *B fragilis* inoculation. Mice were then euthanized, and tumor number (A) and maximum tumor diameter (B) in the mouse colon were assessed. Error bars = SD, n = 5 per group. (C, D) Histologic severity of disease. At the time of euthanasia, colons were fixed in 10% neutral buffered formalin, embedded in paraffin, and stained with hematoxylin and eosin as described in *Methods and Materials* (C). Colons were serially sectioned and degree of dysplasia classified according to the following scale: no dysplasia (0), low grade dysplasia (1), mix of low and high grade dysplasia (2), high grade dysplasia (3) and invasive cancer (4). Examples of no dysplasia (a); low grade dysplasia with pseudo-stratification of the nuclei and nuclear enlargement (b); cribriforming tumor glands significant for high grade dysplasia (c); and surface epithelium with higher grade tumor underneath significant for invasion (d) are shown. Magnification: 20X (D). Error bars = SD. n = 3 per group. Significance: \*, \*\*, \*\*\* denote p < 0.05, 0.01, 0.001, respectively.

CTL. To test this notion, mice with established disease were treated with each cytokine separately or the two cytokines in combination. Analysis of tumor burden in mice that received monotherapy confirmed the beneficial activity of IL-10 while IL-12 increased average tumor number by approximately 30% (Figure 2A). In contrast, combined therapy achieved near-complete tumor elimination in the majority of mice (Figure 2A). A similar trend was observed with regard to tumor size where combination therapy mediated a significant 30% reduction in maximum tumor diameter (Figure 2B). Importantly, and in contrast to treatment with IL-10 alone, histological analysis revealed a dramatic improvement in the pathological score of tumors in mice that received combination therapy (Figure 2C).

The above findings suggested that combined therapy not only arrested tumor growth but actively promoted eradication of established disease. To determine whether IL-10 + IL-12 therapy could provide long-term benefit in this aggressive carcinoma model, mice with established tumors were treated continuously in a survival study. The data shown in Figure 2D demonstrate a 30% increase in median survival in the treatment (93 days) vs the control (71 days) group. Importantly, approximately 30% of the experimental mice remained alive up to and beyond 140 days post-initiation of treatment

(210 days of age), exceeding the maximum lifespan of the APC<sup>min/+</sup> mouse.<sup>21</sup>

Next, we wanted to delineate the cellular mechanism(s) that were responsible for the synergy. Quantitative as well as qualitative analyses of MLN T-cell populations were performed in control vs. treatment groups. Analysis of the IL-10 alone group demonstrated a 35% reduction in the number of CD4+ RORγt+ IL-17+ Th17 cells with no significant impact on CD8+ T-cell activity (Figure 3A). IL-12 monotherapy did not have a detectable effect on Th17 cell numbers but enhanced CTL prevalence and activity. Importantly, combination therapy reduced Th17 cell numbers and increased CTL activity, enhancing the CTL to Th17 cell ratio (Figure 3A). These data demonstrate that each cytokine modulated distinct effector mechanisms in gut-associated immune structures with minimal cross-antagonism.

To determine whether the observed synergy between IL-10 and IL-12 was simply due to enhanced CTL activity in the presence of reduced Th17 prevalence, treatment was performed in the presence or absence of CD8+ T-cell depletion. Analysis of tumor burden revealed that depletion of CD8+ T-cells indeed resulted in reduced antitumor efficacy, though this loss was partial and did not reach statistical significance (Figure 3B). This finding, in combination with the

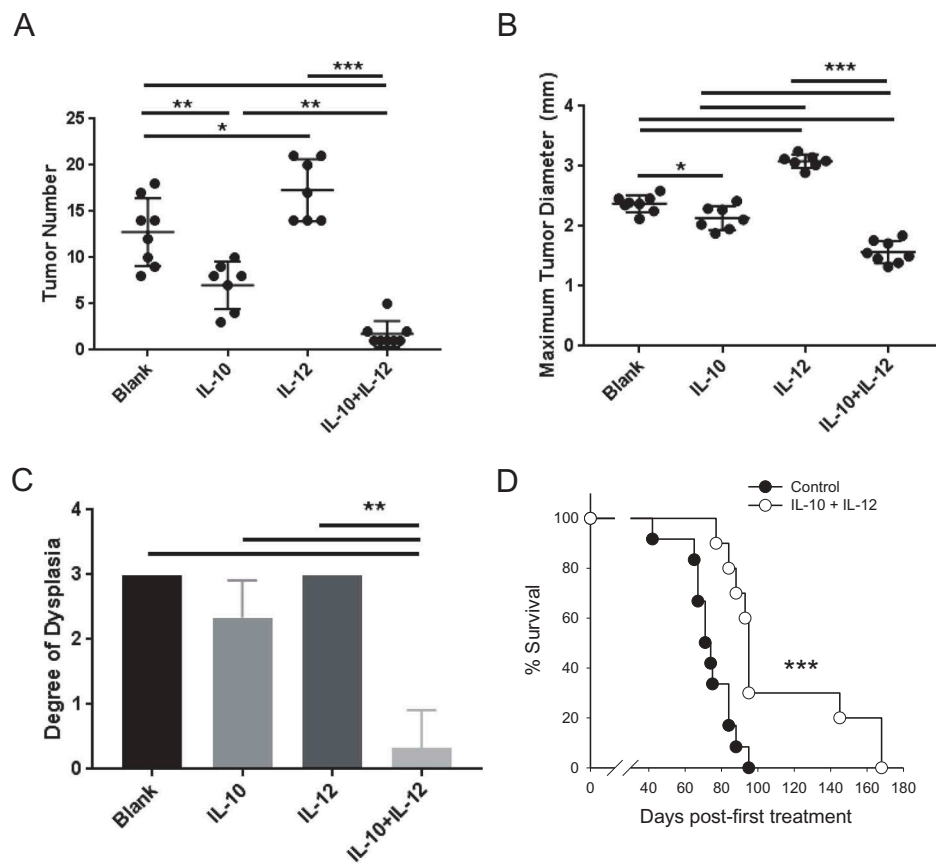


**Figure 2.** Oral IL-10 and IL-12 act synergistically to eradicate established disease and improve overall survival. (A, B) Colon tumor number and maximum diameter. APC<sup>min/+</sup>/B *fragilis* mice were treated with oral particle-based therapy (blank, IL-10, IL-12, or a mixture of IL-10 and IL-12 particles) as in Figure 1. Mice were then euthanized, and tumor number (A) and maximum tumor diameter (B) in the mouse colon were assessed. Error bars = SD, n = 7–8 per group. (C) Histologic severity of disease. At the time of euthanasia, colons were fixed and H&E-stained sections were analyzed as in Figure 1. Error bars = SD, n = 3 per group. (D) Overall survival. APC<sup>min/+</sup>/B *fragilis* mice were treated until euthanasia. n = 12 and 10 for control and experimental groups, respectively. Significance: \*, \*\*, \*\*\* denote p < 0.05, 0.01, 0.001, respectively.

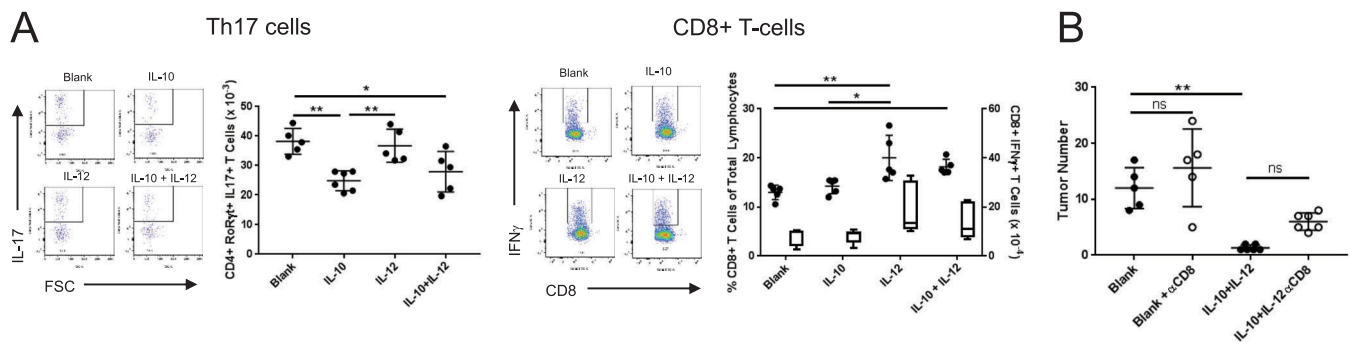


**Figure 3.** Distinct immunological effects of IL-10 and IL-12 on T-cell subsets are partially responsible for the antitumor synergy. (A) Effect of orally administered IL-10 and IL-12 on Th17 and CD8 + T cells. APC<sup>min/+</sup>/B fragilis mice were treated with oral particle-based therapy (blank, IL-10, IL-12, or a mixture of IL-10 and IL-12 particles) as in Figure 1. Mice were euthanized and lymphocytes were isolated from mesenteric lymph nodes. CD4+ RORγt+ cells were gated on and analyzed for IL-17 production (Th17), and CD8 + T cells were analyzed for IFNγ production (CD8 + T-cells) by FACS. Cell numbers shown are per MLN. For CD8 + T-cell panel: filled-in circles = % of total lymphocytes; box plot = number of CD8+ IFNγ+ cells. Boxes have lines at the median plus lower and upper quartiles, with whiskers extending to show the remaining data. Error bars = SD, n = 5 per group. (B) Effect of CD8 + T cell depletion on tumor burden. Tumor-bearing APC<sup>min/+</sup> mice were treated as in Figure 2 in the absence or presence of anti-CD8α monoclonal antibody administration and assessed for tumor burden. Error bars = SD, n = 5–6 per group. Significance: \*, \*\* denote p < 0.05, 0.01, respectively.

independent observation that IL-12 alone actually worsened disease burden, suggested additional mechanisms underpinning the observed synergy.

IL-12 mediates its immunological activity primarily via its immediate downstream effector IFNγ.<sup>23</sup> To obtain further insight into the dichotomous effects of IL-12 in our model, we first investigated the requirement for IFNγ in the pro- vs anti-tumorigenic activity of IL-12 when administered alone or in combination with IL-10, respectively. *In vivo* neutralization of IFNγ in the control and experimental groups demonstrated that blockade of IFNγ activity resulted in the abrogation of both the detrimental and the beneficial activities of IL-12, confirming that both pathways required IFNγ signaling (Figure 4A). This finding suggested that in the combination therapy setting, cooperation between IFNγ and IL-10, two cytokines that are traditionally thought to be antagonistic, was responsible for the unexpected synergy.

In addition to their direct effects on immune effectors, IL-10 and IFNγ are known to reciprocally modulate the paracellular physiology of gut epithelium<sup>24</sup> with potential impact on pro-tumorigenic inflammatory processes.

Specifically, in the APC<sup>min±</sup> model, modulation of gut permeability by DSS<sup>25</sup> results in exacerbation of inflammatory activity and promotes tumorigenesis in the colon.<sup>26</sup> Therefore, to determine whether the IL-10- and/or IL-12-IFNγ-epithelial barrier axis played a role in the observed synergy, we undertook examination of gut epithelial barrier function in different treatment groups. Mice were fed FITC-labeled dextran particles, and serum levels of particles were determined to assess gut permeability in each group. The data show that IL-10 slightly reduced whereas IL-12 substantially enhanced (by 3-fold) permeability compared to that in control mice (Figure 4B). In contrast, co-administration of IL-10 with IL-12 restored serum FITC-dextran levels to steady-state, providing direct evidence that combination therapy had significant impact not only on immune cells but also on the integrity of the gut epithelium. Importantly, neutralization of IFNγ during treatment abrogated the detrimental effect of IL-12 on barrier integrity, mechanistically linking the effects of the IL-12-IFNγ axis on barrier integrity and tumor progression (Figure 4, panels A and C).

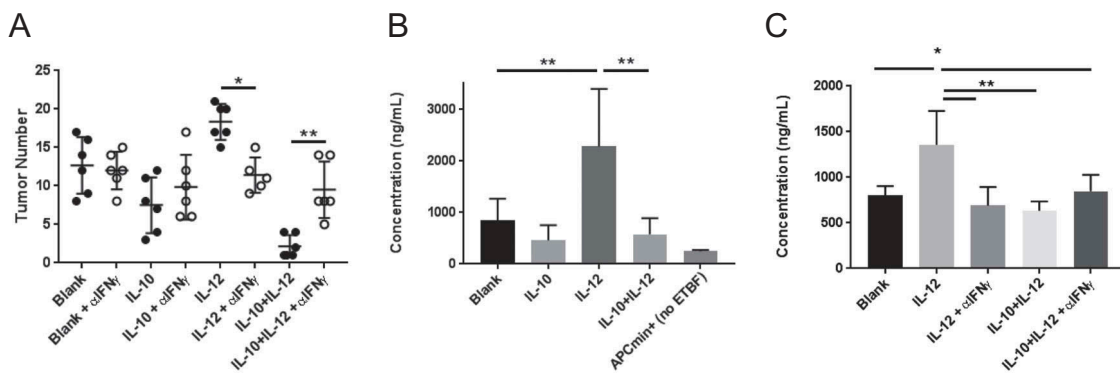


**Figure 4.** Therapeutic synergy requires IFNγ and is in part associated with the effects of cytokines on gut epithelial barrier integrity. (A) Effect of IFNγ neutralization on therapeutic outcome. Tumor-bearing APC<sup>min/+</sup> mice were treated as in Figure 2 in the absence or presence of anti-IFNγ monoclonal antibody administration and assessed for tumor burden. (B) Gut permeability. Experimental mice were administered FITC-labeled dextran via oral gavage at the end of treatment and sera were analyzed for fluorescence to assess leakage as described in Methods and Materials. (C) Effect of IFNγ neutralization on gut permeability. Mice were treated in the absence or presence of IFNγ-neutralizing antibody and sera were analyzed as above. Naïve APC<sup>min/+</sup> mice served as a control for baseline permeability. Error bars = SD, n = 5–6 per group for all studies. Significance: \*, \*\*, \*\*\* denote p < 0.05, 0.01, 0.001, respectively.

We next addressed the mechanism underlying the ability of IL-10 to restore epithelial barrier function in IL-12-treated mice. IL-10 is known to enhance tight junction protein expression in the gut epithelium.<sup>24,27-29</sup> Separately, IFN $\gamma$  was recently shown to induce IL-10RA expression on intestinal epithelial cells.<sup>30</sup> We therefore hypothesized that sensitization of colon epithelium to IL-10 by the IFN $\gamma$ -IL-10RA axis could be responsible for restoration of barrier integrity in mice receiving dual therapy. To this end, we first determined whether oral IL-12 altered IL-10RA expression in the gut. Quantitative PCR analysis revealed that IL-12 promoted 3- and 6-fold increases in IFN $\gamma$  and IL-10RA mRNA expression in the colon, respectively; whereas IL-10 alone had no significant effect (Figure 5A). To determine whether IL-10RA was upregulated on the colon epithelium, we analyzed colon tissue from control and experimental groups by confocal microscopy. The data showed robust IL-10RA expression in the colon epithelium in mice treated with IL-12 or IL-12 + IL-10, whereas no significant protein could be visualized in the control or IL-10 only groups (Figure 5B). We then quantitatively assessed IL-10RA expression on colonic epithelial cells of control vs experimental mice by FACS analysis. These data revealed an approximately 3-fold increase in IL-10RA<sup>+</sup> epithelial cells in the colons of mice that received IL-12 particles (Figure 5C). Collectively, these results supported the

hypothesis that restoration of barrier integrity in mice receiving dual treatment vs IL-12 alone was associated with increased responsiveness of IFN $\gamma$ -conditioned epithelium to exogenous IL-10.

We further pursued the above hypothesis using an *in vitro* colon explant culture system in which the predicted mechanism could be assessed directly. Specifically, we evaluated the effect of cytokine exposure on select tight junction protein levels. To this end, colons of *B fragilis*-infected APC<sup>min/+</sup> mice were incubated in media or media with IL-10, IFN $\gamma$  or IL-10 + IFN $\gamma$ ; and epithelial occludin, claudin-4 and IL-10RA expression were quantified by qPCR and Western blot. The results demonstrated that IFN $\gamma$ , alone or in combination with IL-10, enhanced IL-10RA transcript levels by 8 to 10-fold on average (Figure 6A). Similar increases in both occludin and claudin-4 mRNA were also observed, but only in the combination group (Figure 6A). Western blot analysis revealed a similar trend in protein expression in explants that were exposed to IFN $\gamma$  + IL-10 for all markers (Figure 6B). Collectively, these findings further supported the mechanistic hypothesis that the stromal effect of the cytokines was associated with enhanced tight junction integrity, which required IFN $\gamma$ -dependent sensitization of the epithelium to IL-10.

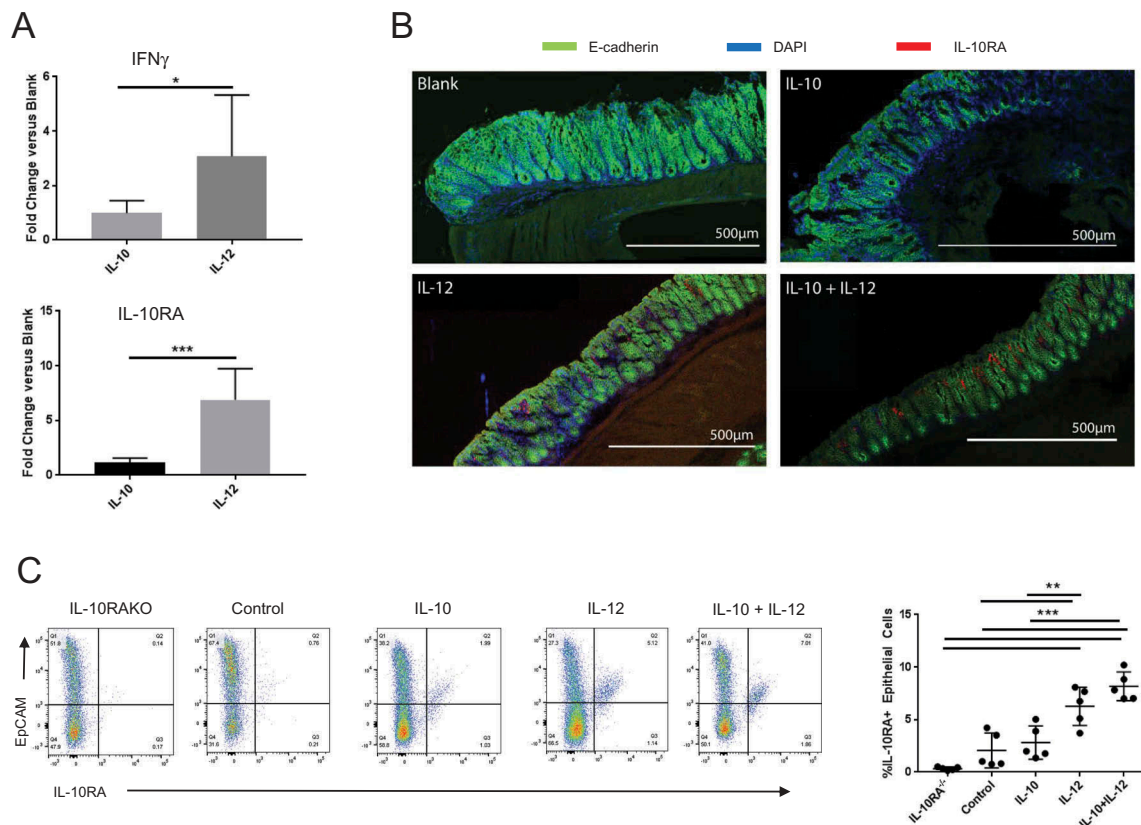


**Figure 5.** IL-12 induces IFN $\gamma$  and IL-10RA expression in the colon. (A) Quantitative PCR analysis of IL-10RA and IFN $\gamma$  mRNA. Quantitative PCR was performed to evaluate relative changes in IL-10RA and IFN $\gamma$  transcript levels in the colon in blank or cytokine particle-treated mice. (B) IL-10RA expression on colon epithelium. Colon sections from control (blank), IL-10, IL-12 and IL-10+ IL-12-treated mice were stained for DAPI (blue), E-cadherin (green), and IL-10RA (red) and visualized by laser-scanning confocal microscopy. (C) FACS analysis of epithelial cell IL-10RA expression. Single cell preparations from colon epithelia of control and treated mice (along with a negative control, i.e. IL-10RA knockout wild-type B6 mice) were stained for EpCAM and IL-10RA expression and were analyzed by flow cytometry. Representative panels and quantitative data are shown. Each circle indicates an individual mouse. Error bars = SD, n = 5 per group. Significance: \*, \*\*, \*\*\* denote p < 0.05, 0.01 and 0.001, respectively.

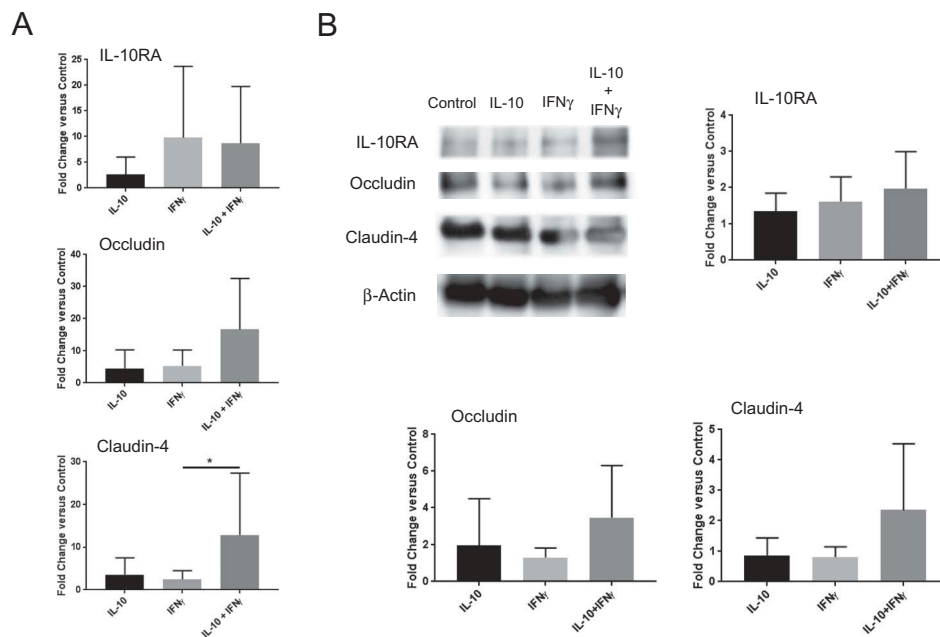


**Figure 6.** IFN $\gamma$  and IL-10 jointly promote tight junction protein expression in the colon. (A) Quantitative PCR analysis of IL-10RA, occludin and claudin-4 transcripts. Colon explants were cultured for 24 hours in high glucose medium in the presence of recombinant IL-10, IFN $\gamma$ , or both as described in *Materials and Methods*. RNA was extracted and IL-10RA, occludin and claudin-4 mRNA levels were quantified by qPCR. Error bars = SD, n = 6 per group. (B, C) Analysis of protein levels. Protein was extracted from colon explants cultured as above and analyzed by Western blotting to detect and quantify IL-10RA, occludin and claudin-4. (B) Western blot. Representative blot displaying the bands for each protein and  $\beta$ -actin (loading control) is shown. (C) Quantification of protein levels. Signal intensity of each band was normalized to  $\beta$  actin for loading in each lane and fold-change was calculated with respect to untreated (control) explants. Combined data from two different blots are shown. Error bars = SD, n = 5–6 per group. Significance: \* denotes  $p < 0.05$ .

## Discussion

Herein, we demonstrate that oral delivery of IL-10 and IL-12 can effectively eradicate established tumors in the APC<sup>min/+</sup>/*B fragilis* colon cancer model. Further, we provide insight into the mechanisms that underlie the synergy between IL-10 and IL-12, two conventionally-antagonistic cytokines. Specifically, we found that, in addition to their distinct immunological effects on Th17 and CTL activity, combined administration of IL-10 and IL-12 improved gut barrier integrity via the IFN $\gamma$ -IL-10RA axis, greatly enhancing therapeutic outcome. These findings have important clinical implications for immune-based therapy of colon cancer, which has traditionally been resistant to this modality.

The primary immunological effects of IL-10 and IL-12 involved distinct activities on Th17 and CD8 + T-cell activity, respectively. Specifically, IL-10 diminished the prevalence of IL-17-producing CD4+ ROR $\gamma$ t+ Th17 cells consistent with our previous observations.<sup>21,22</sup> IL-12, on the other hand, enhanced IFN $\gamma$ -producing CD8 + T-cell numbers. Importantly, these activities were independent and were not antagonistic. We hypothesize that the lack of antagonism between the two cytokines was associated with the distinct and in some cases opposing effects of IL-10 on T-cells of different ontogeny and maturation stage. Specifically, while IL-10 is known to globally suppress T-effector cell priming via its tolerogenic activity on antigen-presenting cells,<sup>12–15</sup> recent data are consistent with differential effects on antigen-experienced effector subsets. For example, while IL-10 can directly suppress Th17 effector cell expansion,<sup>16</sup> multiple reports have confirmed its ability to enhance the activity of primed CD8 + T-cells.<sup>18–20,22</sup> Conversely, the suppression of IL-10 production by IFN $\gamma$ , the

downstream effector of IL-12, occurs at the level of transcription<sup>31</sup> and delivery of recombinant IL-10 would bypass such a mechanism. It is therefore likely that these selective effects on terminally-differentiated T-effector cell subsets underlie the lack of immunological antagonism between the two cytokines in our system.

An unexpected finding in this study was that the sensitization of the gut epithelium to IL-10 by IL-12 was ultimately responsible for the greater part of the synergistic antitumor effect. Whereas our data demonstrate a link between barrier function and therapeutic outcome, they do not directly address the mechanistic basis of how loss of barrier integrity led to increased tumor growth. It is well known that disruption of gut epithelial barrier can promote tumor growth via complex multi-pathway inflammatory processes that involve both microbial as well as non-microbial factors.<sup>32,33</sup> Specifically, both type 17 and type 1 T-cell activity, as well as innate inflammatory cells can contribute to tumor growth in the inflamed gut.<sup>32,33</sup> In the case of the APC<sup>min/+</sup>/*B fragilis* model microbially-driven type 17 immunity has been shown to be essential to tumor development.<sup>8,22,34</sup> While our findings are consistent with this paradigm, the ability of IL-12 to exacerbate disease without significant impact on Th17 cells suggests that additional, yet unidentified, factors that are associated with increased gut permeability may also contribute to tumor pathogenesis in this model.

Our data provide partial insight into the molecular mechanism(s) that underlie the combined effects of IL-12 and IL-10 on barrier function. Consistent with previous reports, IL-12, through its downstream effector IFN $\gamma$ , upregulated IL-10RA expression in the colon epithelium *in vivo* and *in vitro*. Importantly, combined treatment of colon explants with IFN $\gamma$

+ IL-10 induced the expression of tight junction proteins occludin and claudin-4. Collectively, these observations support the hypothesis that increased IL-10 signaling in the IFN $\gamma$ -conditioned gut epithelium ultimately restored barrier integrity via enhanced tight junction formation. In this study, we examined only two tight junction proteins that are known to be critical to barrier function. Given the variety and the complexity of tight junction protein family, a more detailed analysis of the global changes in tight junction protein levels as well as spatial localization could further delineate the molecular pathways underlying the observed effect. A question that remains is how IL-10 signaling overcame the detrimental activity of IFN $\gamma$  in the combination therapy group. IL-10 and IFN $\gamma$  can cross-modulate each other's signaling pathways.<sup>30,35</sup> Whether the dominance of one over the other is determined simply via the relative strength of STAT1 vs STAT3 signaling, and/or through additional pathways remains to be determined.

The above findings demonstrate that colon physiology can be effectively modulated by orally-administered slow-release cytokine formulations, establishing further proof-of-principle for the clinical potential of this therapy. This strategy provides the advantages that drugs can be delivered in a tissue-specific manner to achieve sustained physiological levels in the disease microenvironment with minimal systemic toxicity. We have in the past, demonstrated similar success with oral cytokine formulations in models of IBD, intestinal polyposis and colon cancer.<sup>21,22,36</sup> The current data not only confirm and extend previous findings but also further identify a novel therapeutic modality involving the synergistic use of two traditionally antagonistic cytokines.

## Materials and methods

### Mice and the tumor model

C57BL/6 (B6), C57BL/6J-Apc<sup>Min</sup>/J (APC<sup>Min/+</sup>) and B69S(JL)-IL-10ra<sup>tm1.1Ttg</sup>/J (IL-10RA knockout) mice were purchased from Jackson Laboratory. Enterotoxigenic *B fragilis* strain 86-5443-2-2 was a kind gift from Dr. Cynthia L Sears (Johns Hopkins University School of Medicine, Baltimore, Maryland). For colonization with *B fragilis*, 5–6 week old APC<sup>Min/+</sup> mice were administered clindamycin (0.1g/L) and streptomycin (5g/L) *ad libitum* in drinking water for 5 days before oral gavage (~5 × 10<sup>7</sup> bacteria in PBS) as previously described.<sup>8</sup> All studies were conducted in accordance with guidelines set forth by the Institutional Animal Care and Use Committee at the University of Louisville (Louisville, KY).

### Reagents and treatments

Two particle formulations were produced using a modified Phase Inversion Nanoencapsulation (PIN) process:<sup>37</sup> (i) control (no cytokine) and (ii) recombinant murine IL-10 or IL-12-encapsulated (Peprotech, Inc.) with a loading of 0.5  $\mu$ g or 0.25  $\mu$ g cytokine/mg of particles, respectively. Particles were administered via oral gavage (1 mg particles in 0.2 mL sterile water for blank, IL-10, and IL-12 treatments and 2 mL total particles in 0.2 mL sterile water for combination IL-10 and IL-12 treatment) starting 4 weeks after *B fragilis* inoculation three times per week for 3 weeks. Administration of particles resulted in a transient but significant

increase in cytokine levels in the gut lamina propria (Supplemental Figure 1). For survival analysis, mice were treated until they reached the IACUC-approved euthanasia score as previously described by our group.<sup>21</sup>

### Gross intestinal preparation and tumor quantification

Colons were opened longitudinally before being fixed in 10% neutral buffered formalin. Tumor burden was quantified using a dissecting microscope.

### Histology

Formalin-fixed, paraffin-embedded tissue from the distal colon was sectioned serially (5 $\mu$ m sections) and subsequently stained with Hematoxylin and Eosin (H&E). Colon histology was assessed in a blinded fashion by a single tumor pathologist. Each section was classified as harboring no dysplasia, low grade dysplasia, or high grade dysplasia. Colons were then scored according to the following system based on the average severity of dysplasia in the distal colon: 0 – no dysplasia; 1 – low grade dysplasia only; 2 – mixture of low grade and high grade dysplasia; 3 – high grade dysplasia only; 4 – invasive cancer.

### Laser-scanning confocal microscopy

Colon and tumor tissues were harvested from mice, embedded in Tissue-Plus Optimal Cutting Temperature (OCT) Compound (Fisher HealthCare, Houston, TX, USA) and snap-frozen in liquid nitrogen. Serial cryosections (25  $\mu$ m) were prepared with a Cryostar NX70, Thermo Scientific cryostat at -19°C (Kalamazoo, MI, USA). Cryosections were kept at room temperature for at least 24 h prior to staining. A previously described immunostaining protocol was used with modifications.<sup>38</sup> For analysis of IL-10RA expression, staining antibodies were added sequentially in the following order: IL-10RA- phycoerythrin (PE) (Novus Biologicals, Littleton, CO), CD324 (E-Cadherin) Alexa Fluor-488 (Thermo Fisher, Waltham, MA). Sections were washed twice with 1X PBS-T and processed for imaging. For analysis of colon sections, staining antibodies were added sequentially in the following order: IL-10RA- phycoerythrin (PE) (Novus Biologicals, Littleton, CO), CD324 (E-Cadherin) Alexa Fluor-488 (Thermo Fisher, Waltham, MA). Antibodies were diluted with 2% fetal calf serum (FCS) in 1X PBS pH 7.4 to 1:25 for IL-10RA-PE, and 1:25 for CD324 E-Cadherin Alexa Fluor-488. Each antibody was sequentially incubated at 37°C for 40 mins. Sections were washed twice with 1X PBS-T and Prolong Gold anti-fade reagent (Thermo Fisher, Waltham, MA) was added to the slides prior to imaging. Images were captured using a Leica SP5 confocal laser scanning microscope (Leica, Wetzlar, Germany) and processed using Fiji Software.<sup>39</sup> Panels containing confocal images were generated using Adobe Photoshop version 13.0 x32. Images were marked using the drawing tools to highlight the results and to provide orientation of the tissues.

### Colon epithelial cell isolation

Mouse (C57BL/6) colons were excised, flushed with PBS + penicillin and streptomycin (P/S), hemisected longitudinally, and

rinsed with ice cold PBS + P/S. Colons were then cut into 5 mm pieces and placed in a 50 mL conical tube containing 20 mL HBSS + 1 mM DTT + 1 mM EDTA + 5% FBS. Tubes were placed in a hybridization oven and incubated at 200 RPM, 37°C for 40 minutes. Contents were then passed through a 100 µm filter and centrifuged at 1500 RPM for 5 minutes. Supernatant was discarded, and the pellet was subjected to density dependent centrifugation using a 25%-40% discontinuous Percoll gradient. Cells were harvested at the interface of the solutions and placed in 2 mL 100% FBS. Cells were centrifuged again at 1500 RPM for 5 minutes and reconstituted in 2 mL PBS + 0.1% BSA for FACS analysis.

### Flow cytometry

Membrane and intracellular staining of MLN or epithelial cells were performed as described.<sup>22</sup> The following antibodies were used: CD4 (GK1.5, BioLegend), CD8α (53-6.7, BD Biosciences), CD16/CD32 (93, BioLegend), IL-17A (TC11-18H10.1, BioLegend), RORγt (Q31-378, BD Biosciences), IFNγ (XMG1.2, BD Biosciences), IL-10RA (1B1.3a, BioLegend), and Ep-CAM (G8.8, BioLegend).

### Lymphocyte depletion and functional blockade studies

Anti-mouse CD8α (53-6.72, BioXCell) was given intraperitoneally (ip) to APC<sup>min/+</sup> mice (0.2mg, three times per week for 3 weeks) to deplete CD8 + T lymphocytes. Anti-mouse IFNγ (XMG1.2, BioXCell) was injected ip (0.2mg, three times per week for 3 weeks). All treatments were initiated on treatment day -1 (the day before receiving their first oral immunotherapy treatment) and again on treatment day 0 (the day of their first oral immunotherapy treatment). Mice were subsequently treated IP twice weekly for the duration of their 3 week oral immunotherapy treatment regimen.

### Colon permeability study

Colon permeability was assessed using a FITC-dextran assay as previously described.<sup>40</sup> Briefly, APC<sup>min/+</sup>/*B fragilis* mice were treated with oral immunotherapy as described above. After 3 weeks of treatment, they were water starved overnight before being gavaged with 44 mg/100 g body weight of FITC labeled dextran (FD4, Millipore Sigma, St. Louis, Missouri, USA) suspended in sterile PBS at a concentration of 100 mg/mL. After a period of 4 hours, 300 mL of blood was extracted retro-orbitally and placed in a BD SST collection tube (BD, Franklin Lakes, New Jersey, USA). After centrifugation, serum was aspirated and diluted 1:1 with sterile PBS. Samples were pipetted into a 96-well plate and analyzed using a plate reader (em: 485 nm, ex: 526 nm). Concentration of FITC-dextran was calculated based upon a standard curve.

### Colon explant culture

Colon tissue pieces (0.5–1 cm length) from APC<sup>min/+</sup>/*B fragilis* mice were cultured in triplicates for 24 hours in complete DMEM-high glucose medium (supplemented with 10% fetal bovine serum, 1X penicillin-streptomycin solution) in a humidified atmosphere (37°C, 5% CO<sub>2</sub>) in the presence of

recombinant murine IL-10 (30 ng/mL, PeproTech, Rocky Hill, New Jersey, USA), recombinant murine IFNγ (20 ng/mL, PeproTech, Rocky Hill, New Jersey, USA), or a combination of recombinant murine IL-10 and IFNγ. The tissues were processed for protein preparation (tissue lysates with RIPA buffer) using a sonic dismembrator (Model 550, Fisher Scientific). These tissue lysates were used to determine the expression of IL-10RA, claudin-4, and occludin.

### Western blots

Total protein lysates were collected either from colon tissue or colon epithelial cells as described above using radioimmunoprecipitation assay (RIPA) buffer (Millipore Sigma, St. Louis, Missouri, USA) and quantified using BCA protein quantification kit (Thermo Fisher Scientific, Waltham, Massachusetts, USA) per instructional manual. Total protein (20–50 µg) of was resolved on Mini-PROTEAN TGX 4–20% gels (Bio-Rad, Hercules, California, USA) and transferred to polyvinylidene difluoride membrane (0.22 µm pore; Novex, Carlsbad, California, USA). After blocking with 3% (w/v) bovine serum albumin (BSA) (containing 1X TBS) for 1 h, the membrane was then incubated with HRP-conjugated anti-claudin-4, anti-occludin, anti-IL-10RA and anti-β-actin antibodies (1:500, 1:500, 1:300 and 1:20,000 dilution, respectively) at 4° C overnight. For all proteins, chemiluminescent substrate (SuperSignal<sup>TM</sup> West Femto Maximum Sensitivity Substrate, Thermo Scientific, Rockford, Illinois, USA) was used to detect the protein bands (ImageQuant LAS 4000). Densitometry analysis of bands was done using ImageJ software. Antibodies for claudin-4, occludin and β-actin were purchased from Santa Cruz Biotechnologies (USA). The antibody for IL-10RA was purchased from Novus Biologicals (USA).

### Quantitative PCR

Steady-state mRNA levels in colon tissue were detected with SYBR Green PCR Master Mix (Applied Biosystems) using the Mx3000p qPCR system (Agilent Technologies). Results were normalized to β-actin expression. The expression level was scaled using the 2<sup>-ΔΔCT</sup> method, with the average levels obtained for colons of APC<sup>min/+</sup>/*B fragilis* mice treated with blank (control) microparticles set arbitrarily to 1. Primer sequences utilized were: β-actin forward 5'-TCACCCACACTGGCCCATCTACGA-3', reverse 5'-TGGTGAAGCTGTAGCCACGCT-3'; IL-10RA forward 5'-GCCAAGCCCTTCCTATGTGT-3', reverse 5'-C CAGGGTGAACGTTGTGAGA-3'; IFNγ forward 5'-GGCA CAGTCATTGAAAGC-3', reverse 5'-TGCCAGTTCCTCCAG ATA-3'; claudin-4 forward 5'-ATGGCGTCTATGGGAC TACA-3', reverse 3'-TTACACATAGTTGCTGGCGG-5'; occludin forward 5'- CCTCCAATGGCAAAGTGAAT-3', reverse 3'-CTCCCCACCTGTCGTGTAGT-5'.

### Statistical analysis

Two-tailed student's t-test was used to determine the significance of the differences between control and experimental groups in pairwise comparisons. In experiments with multiple groups homogeneity of inter-group variance was analyzed by one-way



ANOVA with Tukey's honest standard difference for multiple comparisons. Log-rank test was utilized for analysis of survival studies. *P* values of 0.05 or less were considered statistically significant. Statistical analyses were performed using GraphPad Prism 7 (GraphPad Software, La Jolla, California, USA) and MedCalc version 17.9.7 (MedCalc Software, Ostend, Belgium).

## Funding

The work was supported by the US National Institutes of Health (R01-CA100656, N.K.E.), the University of Louisville start-up funds (N.K.E.) and the University at Albany and Wadsworth Center, New York State Department of Health start-up funds (M.D.J.); HHS | NIH | National Cancer Institute (NCI) [CA100656].

## References

- Ribas A, Wolchok JD. Cancer immunotherapy using checkpoint blockade. *Science*. 2018;359(6382):1350–1355. doi:10.1126/science.aar4060.
- Queirolo P, Spagnolo F. Atypical responses in patients with advanced melanoma, lung cancer, renal-cell carcinoma and other solid tumors treated with anti-PD-1 drugs: A systematic review. *Cancer Treat Rev*. 2017;59:71–78. doi:10.1016/j.ctrv.2017.07.002.
- Boland PM, Ma WW. Immunotherapy for Colorectal Cancer. *Cancers (Basel)*. 2017;9(5). doi:10.3390/cancers9050050.
- Zhang K, Hornef MW, Dupont A. The intestinal epithelium as guardian of gut barrier integrity. *Cell Microbiol*. 2015;17(11):1561–1569. doi:10.1111/cmi.12501.
- De Souza HS, Fiocchi C. Immunopathogenesis of IBD: current state of the art. *Nat Rev Gastroenterol Hepatol*. 2016;13(1):13–27. doi:10.1038/nrgastro.2015.186.
- Kang M, Martin A. Microbiome and colorectal cancer: unraveling host-microbiota interactions in colitis-associated colorectal cancer development. *Semin Immunol*. 2017;32:3–13. doi:10.1016/j.smim.2017.04.003.
- Grivennikov SI, Wang K, Mucida D, Stewart CA, Schnabl B, Jauch D, Taniguchi K, Yu GY, Osterreicher CH, Hung KE, et al. Adenoma-linked barrier defects and microbial products drive IL-23/IL-17-mediated tumour growth. *Nature*. 2012;491(7423):254–258. doi:10.1038/nature11465.
- Wu S, Rhee KJ, Albesiano E, Rabizadeh S, Wu X, Yen HR, Huso DL, Brancati FL, Wick E, McAllister F, et al. A human colonic commensal promotes colon tumorigenesis via activation of T helper type 17 T cell responses. *Nat Med*. 2009;15(9):1016–1022. doi:10.1038/nm.2015.
- Blatner NR, Mulcahy MF, Dennis KL, Scholtens D, Bentrem DJ, Phillips JD, Ham S, Sandall BP, Khan MW, Mahvi DM, et al. Expression of RORgammat marks a pathogenic regulatory T cell subset in human colon cancer. *Sci Transl Med*. 2012;4(164):164ra159. doi:10.1126/scitranslmed.3004566.
- Wang K, Kim MK, Di Caro G, Wong J, Shalapour S, Wan J, Zhang W, Zhong Z, Sanchez-Lopez E, Wu LW, et al. Interleukin-17 receptor a signaling in transformed enterocytes promotes early colorectal tumorigenesis. *Immunity*. 2014;41(6):1052–1063. doi:10.1016/j.immuni.2014.11.009.
- Le Gouvello S, Bastuji-Garin S, Aloulou N, Mansour H, Chaumette MT, Berrehar F, Seikour A, Charachon A, Karoui M, Leroy K, et al. High prevalence of Foxp3 and IL17 in MMR-proficient colorectal carcinomas. *Gut*. 2008;57(6):772–779. doi:10.1136/gut.2007.123794.
- Sabat R, Grutz G, Warszawska K, Kirsch S, Witte E, Wolk K, Geginat J. Biology of interleukin-10. *Cytokine Growth Factor Rev*. 2010;21(5):331–344. doi:10.1016/j.cytogfr.2010.09.002.
- Shouval DS, Biswas A, Goettel JA, McCann K, Conaway E, Redhu NS, Mascanfroni ID, Al Adham Z, Lavoie S, Ibourk M, et al. Interleukin-10 receptor signaling in innate immune cells regulates mucosal immune tolerance and anti-inflammatory macrophage function. *Immunity*. 2014;40(5):706–719. doi:10.1016/j.immuni.2014.03.011.
- Zigmond E, Bernshtein B, Friedlander G, Walker CR, Yona S, Kim KW, Brenner O, Krauthgamer R, Varol C, Muller W, et al. Macrophage-restricted interleukin-10 receptor deficiency, but not IL-10 deficiency, causes severe spontaneous colitis. *Immunity*. 2014;40(5):720–733. doi:10.1016/j.immuni.2014.03.012.
- Ip WKE, Hoshi N, Shouval DS, Snapper S, Medzhitov R. Anti-inflammatory effect of IL-10 mediated by metabolic reprogramming of macrophages. *Science*. 2017;356(6337):513–519. doi:10.1126/science.aal3535.
- Huber S, Gagliani N, Esplugues E, O'Connor W Jr., Huber FJ, Chaudhry A, Kamanaka M, Kobayashi Y, Booth CJ, Rudensky AY, et al. Th17 cells express interleukin-10 receptor and are controlled by Foxp3(-) and Foxp3+ regulatory CD4+ T cells in an interleukin-10-dependent manner. *Immunity*. 2011;34(4):554–565. doi:10.1016/j.immuni.2011.01.020.
- Chaudhry A, Samstein RM, Treuting P, Liang Y, Pils MC, Heinrich JM, Jack RS, Wunderlich FT, Bruning JC, Muller W, et al. Interleukin-10 signaling in regulatory T cells is required for suppression of Th17 cell-mediated inflammation. *Immunity*. 2011;34(4):566–578. doi:10.1016/j.immuni.2011.03.018.
- Mumm JB, Emmerich J, Zhang X, Chan I, Wu L, Mauze S, Blaisdell S, Basham B, Dai J, Grein J, et al. IL-10 elicits IFN $\gamma$ -dependent tumor immune surveillance. *Cancer Cell*. 2011;20(6):781–796. doi:10.1016/j.ccr.2011.11.003.
- Emmerich J, Mumm JB, Chan IH, LaFace D, Truong H, McClanahan T, Gorman DM, Oft M. IL-10 directly activates and expands tumor-resident CD8(+) T cells without de novo infiltration from secondary lymphoid organs. *Cancer Res*. 2012;72(14):3570–3581. doi:10.1158/0008-5472.can-12-0721.
- Chan IH, Wu V, Bilardello M, Mar E, Oft M, Van Vlasselaer P, Mumm JB. The Potentiation of IFN- $\gamma$  and Induction of Cytotoxic Proteins by Pegylated IL-10 in Human CD8 T Cells. *J Interferon Cytokine Res*. 2015;35(12):948–955. doi:10.1089/jir.2014.0221.
- Chung AY, Li Q, Blair SJ, De Jesus M, Dennis KL, LeVea C, Yao J, Sun Y, Conway TF, Virtuoso LP, et al. Oral interleukin-10 alleviates polyposis via neutralization of pathogenic T-regulatory cells. *Cancer Res*. 2014;74(19):5377–5385. doi:10.1158/0008-5472.can-14-0918.
- Gu T, De Jesus M, Gallagher HC, Burris TP, Egilmez NK. Oral IL-10 suppresses colon carcinogenesis via elimination of pathogenic CD4(+) T-cells and induction of antitumor CD8(+) T-cell activity. *Oncimmunology*. 2017;6(6):e1319027. doi:10.1080/2162402x.2017.1319027.
- Trinchieri G. Interleukin-12 and the regulation of innate resistance and adaptive immunity. *Nat Rev Immunol*. 2003;3(2):133–146. doi:10.1038/nri1001.
- Capaldo CT, Nusrat A. Cytokine regulation of tight junctions. *Biochim Biophys Acta*. 2009;1788(4):864–871. doi:10.1016/j.bbame.2008.08.027.
- Brandl K, Rutschmann S, Li X, Du X, Xiao N, Schnabl B, Brenner DA, Beutler B. Enhanced sensitivity to DSS colitis caused by a hypomorphic *Mbtps1* mutation disrupting the ATF6-driven unfolded protein response. *Proc Natl Acad Sci U S A*. 2009;106(9):3300–3305. doi:10.1073/pnas.0813036106.
- Tanaka T, Kohno H, Suzuki R, Hata K, Sugie S, Niho N, Sakano K, Takahashi M, Wakabayashi K. Dextran sodium sulfate strongly promotes colorectal carcinogenesis in *Apc(Min/+)* mice: inflammatory stimuli by dextran sodium sulfate results in development of multiple colonic neoplasms. *Int J Cancer*. 2006;118(1):25–34. doi:10.1002/ijc.21282.
- Oshima T, Laroux FS, Coe LL, Morise Z, Kawachi S, Bauer P, Grisham MB, Specian RD, Carter P, Jennings S, et al. Interferon- $\gamma$  and interleukin-10 reciprocally regulate endothelial junction integrity and barrier function. *Microvasc Res*. 2001;61(1):130–143. doi:10.1006/mvre.2000.2288.

28. Madsen KL, Lewis SA, Tavernini MM, Hibbard J, Fedorak RN. Interleukin 10 prevents cytokine-induced disruption of T84 monolayer barrier integrity and limits chloride secretion. *Gastroenterology*. 1997;113(1):151–159.
29. Sun X, Yang H, Nose K, Nose S, Haxhija EQ, Koga H, Feng Y, Teitelbaum DH. Decline in intestinal mucosal IL-10 expression and decreased intestinal barrier function in a mouse model of total parenteral nutrition. *Am J Physiol Gastrointest Liver Physiol*. 2008;294(1):G139–147. doi:10.1152/ajpgi.00386.2007.
30. Kominsky DJ, Campbell EL, Ehrentraut SF, Wilson KE, Kelly CJ, Glover LE, Collins CB, Bayless AJ, Saeedi B, Dobrinskikh E, et al. IFN- $\gamma$ -mediated induction of an apical IL-10 receptor on polarized intestinal epithelia. *J Immunol*. 2014;192(3):1267–1276. doi:10.4049/jimmunol.1301757.
31. Schaefer A, Unterberger C, Frankenberger M, Lohrum M, Staples KJ, Werner T, Stunnenberg H, Ziegler-Heitbrock L. Mechanism of interferon-gamma mediated down-regulation of interleukin-10 gene expression. *Mol Immunol*. 2009;46(7):1351–1359. doi:10.1016/j.molimm.2008.11.015.
32. Luissint AC, Parkos CA, Nusrat A. Inflammation and the Intestinal Barrier: leukocyte-Epithelial Cell Interactions, Cell Junction Remodeling, and Mucosal Repair. *Gastroenterology*. 2016;151(4):616–632. doi:10.1053/j.gastro.2016.07.008.
33. Lechuga S, Ivanov AI. Disruption of the epithelial barrier during intestinal inflammation: quest for new molecules and mechanisms. *Biochim Biophys Acta*. 2017;1864(7):1183–1194. doi:10.1016/j.bbamcr.2017.03.007.
34. Thiele Orberg E, Fan H, Tam AJ, Dejea CM, Destefano Shields CE, Wu S, Chung L, Finard BB, Wu X, Fathi P, et al. The myeloid immune signature of enterotoxigenic *Bacteroides fragilis*-induced murine colon tumorigenesis. *Mucosal Immunol*. 2017;10(2):421–433. doi:10.1038/mi.2016.53.
35. Ito S, Ansari P, Sakatsume M, Dickensheets H, Vazquez N, Donnelly RP, Larner AC, Finbloom DS. Interleukin-10 inhibits expression of both interferon alpha- and interferon gamma-induced genes by suppressing tyrosine phosphorylation of STAT1. *Blood*. 1999;93(5):1456–1463.
36. Conway TF, Hammer L, Furtado S, Mathiowitz E, Nicoletti F, Mangano K, Egilmez NK, Auci DL. Oral Delivery of Particulate Transforming Growth Factor Beta 1 and All-Trans Retinoic Acid Reduces Gut Inflammation in Murine Models of Inflammatory Bowel Disease. *J Crohns Colitis*. 2015;9(8):647–658. doi:10.1093/ecco-jcc/jjv089.
37. Egilmez NK, Jong YS, Mathiowitz E, Bankert RB. Tumor vaccination with cytokine-encapsulated microspheres. In: Driscoll B, editor. Vol 75: Lung Cancer; Vol 2: Diagnostic and Therapeutic Methods and Reviews Methods in Molecular Medicine. Totowa (NY): Humana Press; 2003. p. 687–696.
38. De Jesus M, Ahlawat S, Mantis NJ. Isolating and immunostaining lymphocytes and dendritic cells from murine Peyer's patches. *J Vis Exp*. 2013;(73). doi:10.3791/50167.
39. Schindelin J, Arganda-Carreras I, Frise E, Kaynig V, Longair M, Pietzsch T, Preibisch S, Rueden C, Saalfeld S, Schmid B. Fiji: an open-source platform for biological-image analysis. *Nat Methods*. 2012;9(7):676. doi:10.1038/nmeth.2019.
40. Gupta J, Nebreda AR. Analysis of intestinal permeability in mice. *Bio-protocol*. 2014;4(22). doi:10.21769/BioProtoc.1289.